Detection of Extragalactic Radio Source VIRGO A with Amateur Radio Astronomy Equipment

1 Introduction

This article describes the detection of an extragalactic radio object known as Virgo A during February 2008 using an amateur interferometer at 406MHz.

Virgo A is a giant elliptical galaxy - Messier 87 (NGC 4486, 3C274) and is one of the most remarkable objects in the sky. It is perhaps the largest galaxy in the closest big cluster to us, the famous Virgo Cluster of galaxies (sometimes called "Coma-Virgo cluster" and lies at the distance of this cluster (about 60 million light-years). The cluster is shown in Figure 1.

The galaxy is over half a degree in extent (more than the diameter of the full moon) as shown in long exposure photographs[1] and this corresponds to a linear diameter of more than half a million light years -. Its coordinates are $12^h\ 30^m\ 49.42338^s$ RA and +12° 23′ 28.0439″ Dec.

Figure 1 The Virgo cluster of Galaxies

M87's apparent core diameter is about 7' and corresponds to 120,000 light years - more than the diameter of our Milky Way's disk.

However, as M87 is of type E1 or E0, it fills a much larger volume, and thus contains many more stars (and mass) than our galaxy - certainly several trillion (10^12) solar masses [2].

M87 was identified with the radio source Virgo A by W. Baade and R. Minkowski in 1954. In 1956, a weaker radio halo was found by J.E. Baldwin and F.G. Smith of Cambridge. The galaxy has a spectacular jet which is better seen on short exposure photographs as shown in Figure 2. This is a directional beam of relativistic[+] plasma issuing from the core of the galaxy and contributes to its radio emissions.

Figure 2 Virgo A relativistic jet

The jet is thought to be produced by a violent active nucleus in the galaxy, probably a massive central object of several billion solar masses concentrated within the innermost sphere with a radius of 60 light years.

It is probable that at the core of this galaxy is a super-massive black hole (SMBH) with an estimated $(6.6 \pm 0.4) \times 10^9$ times the mass of the Sun and a diameter larger than the orbit of Pluto. This is one of the highest masses known for such an object. Surrounding the black hole is a rotating disk of ionized gas that is oriented roughly perpendicular to the jet. This gas is moving at velocities of up to roughly 1,000 km/s [3]. Gas is accreting onto the black hole at an estimated rate equal to the mass of the Sun every ten years [4].

[+] Moving at speeds close to the speed of light

An impression of the accretion disc and the plasma jets associated with the super-massive black hole is shown in Figure 3. Here both jets are shown, but in the actual optical image of M87 in Figure 2, only the forward jet can be seen, presumably due to obscuration of the rearward jet by the galaxy itself.

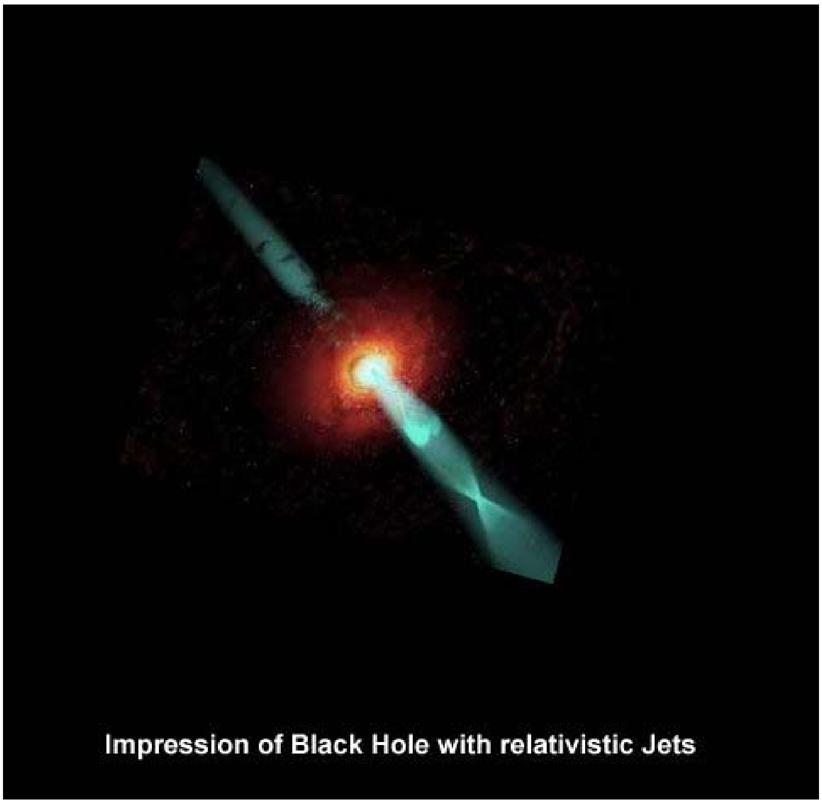

Figure 3 Impression of jets from a super-massive black hole

The detection of this object by amateur radio astronomers is a challenge as it has a strength of only ~ 560Jy at 406MHz. (1Jy = 10^{-26} W/m^2).

Table1 Flux levels for Virgo A

Freq: 38 MHz	Flux: 3200 Janskys
Freq: 178 MHz	Flux: 970 Janskys
Freq: 240 MHz	Flux: 800 Janskys
Freq: 408 MHz	Flux: 519 Janskys
Freq: 412 MHz	Flux: 500 Janskys
Freq: 958 MHz	Flux: 300 Janskys
Freq: 1420 MHz	Flux: 200 Janskys
Freq: 2700 MHz	Flux: 120 Janskys
Freq: 3200 MHz	Flux: 100 Janskys
Freq: 5000 MHz	Flux: 67.6 Janskys

The calculated Spectral Index: 0.79 *

*Radio Eyes

Table 2 Flux levels for Cygnus A 3C405

Freq: 38 MHz	Flux: 22000 Janskys
Freq: 178 MHz	Flux: 8700 Janskys
Freq: 408 MHz	Flux: 4700 Janskys
Freq: 710 MHz	Flux: 2800 Janskys
Freq: 958 MHz	Flux: 2100 Janskys
Freq: 1420 MHz	Flux: 1500 Janskys
Freq: 3200 MHz	Flux: 600 Janskys

Calculated Spectral Index: 0.81

Table 3 Flux levels for Cassiopeia A 3C461

Freq: 38 MHz	Flux: 36000 Janskys
Freq: 178 MHz	Flux: 11000 Janskys
Freq: 240 MHz	Flux: 8500 Janskys
Freq: 408 MHz	Flux: 5500 Janskys
Freq: 412 MHz	Flux: 5300 Janskys
Freq: 710 MHz	Flux: 4000 Janskys
Freq: 958 MHz	Flux: 2900 Janskys
Freq: 1420 MHz	Flux: 2400 Janskys
Freq: 3200 MHz	Flux: 1300 Janskys

Calculated Spectral Index: 0.75

Table 4 Comparison of radio sources at 408MHz

Virgo A	519 Janskys
Cygnus A	4700 Janskys
Cassiopeia A	5500 Janskys

It is obvious that there is a significant difference in flux from Virgo A and these bright sources (Cassiopeia and Cygnus) which are the usual targets for amateur radio astronomers. Virgo A is an order of magnitude weaker than these other sources.

To reliably detect Virgo A, the amateur radio astronomer must take special care with the stability of the equipment being used to make these small signal measurements. The best (lowest noise) results may be obtained by combining measurements made on different days requiring a high level of receiver stability. This necessitates temperature controlled Low Noise Amplifiers (LNAs), cable line drivers and receiver.

In what follows the equipment used to detect Virgo A is described and results are presented.

2 Measurement Technique

2.1 Source angular diameter

Virgo A is an extra-galactic object with an angular diameter much smaller than the basic radio features of the Milky Way such as the distribution of broad spectrum synchrotron emission or the narrow 'line emission' from neutral hydrogen. (Amateur measurements of these can also be found on the RAG web site).

If a small low intensity source such as Virgo A is to be 'picked out' of the general galactic background, a narrow antenna beam is required or the integrated galactic background signal over the antenna beam will swamp the object which we desire to detect.

At 408 MHz this requires a large aperture antenna, many metres in diameter and which is usually beyond the resources of the amateur. It is however possible to produce a narrow beam using an interferometer arrangement. This may well be within the scope of the amateur to construct and operate.

2.2 A two element Interferometer

Descriptions of a radio interferometer can be found in many publications [5 6] and show how, by separating two or more antennas by many wavelengths (at which observations are being made) it is possible to create - or synthesise - a number of antenna beams with narrow beamwidth: much narrower in fact than the beamwidth of the individual antennas used in the array. The explanation given below demonstrates this feature.

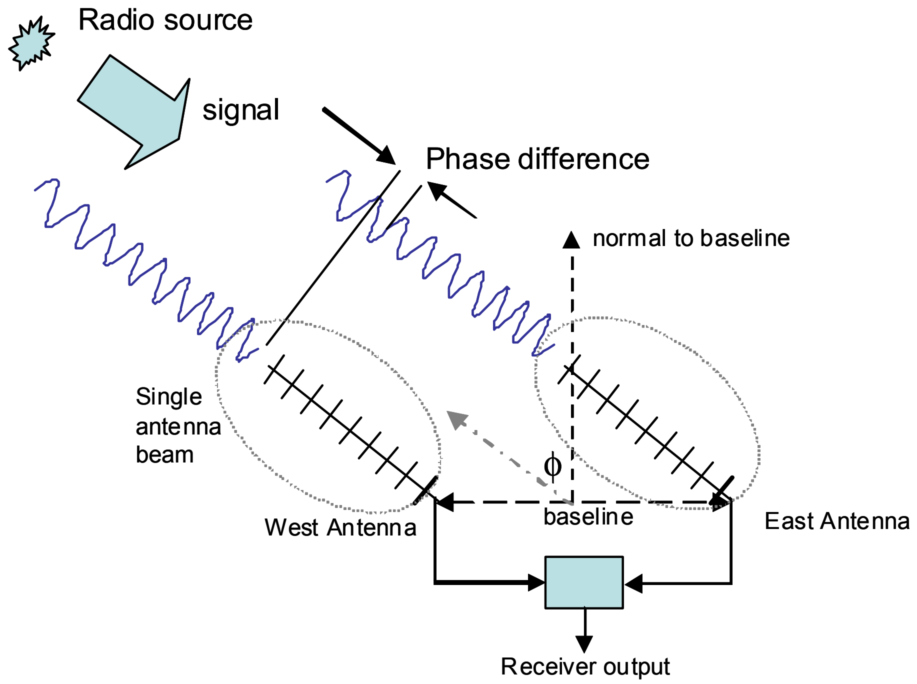

Figure 4 A basic two antenna Interferometer

The signal arriving from a source at some angle ϕ to the normal to the baseline reaches the two antennas at slightly different times. This represents a difference in the phase of the signals with respect to each other. Thus at some angles the two waves may be in phase – doubling the strength of the received signal – and at other angles they will be out of phase cancelling each other, resulting in no signal. As the source moves across the sky the angle of incidence ϕ changes and the signal level varies between maximum and zero several times as it passes through the relatively wide beam of a single antenna.

The angle between successive maxima is given by:

$$\theta = 57.3\ \lambda / D$$

Where θ = interferometer pattern angular resolution
λ= wavelength in m
D= length of baseline in m

For the interferometer used to make measurements of Virgo A in this report the wavelength used was 0.738m and the baseline was 30m long. This results in an angular resolution of 1.4 degrees. The half power or 3dB beamwidth will be somewhat smaller than this. Figure 5 shows how the interferometer produces a series of fine beams along an E-W axis, with the intensity falling off both E-W and N-S due to the beam shape of a single antenna

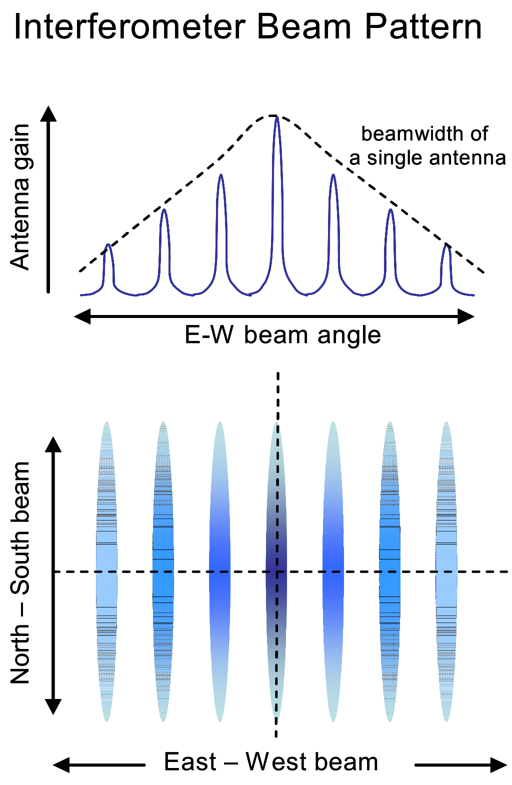

Figure 5 Interferometer beam pattern

The actual interferometer used in these measurements is shown in Figure 6. Each antenna is made from two 16dB gain SARA* quagi [7] antennas to provide a narrow 'single antenna' beam and extra gain.

The construction of these antennas will be described below.

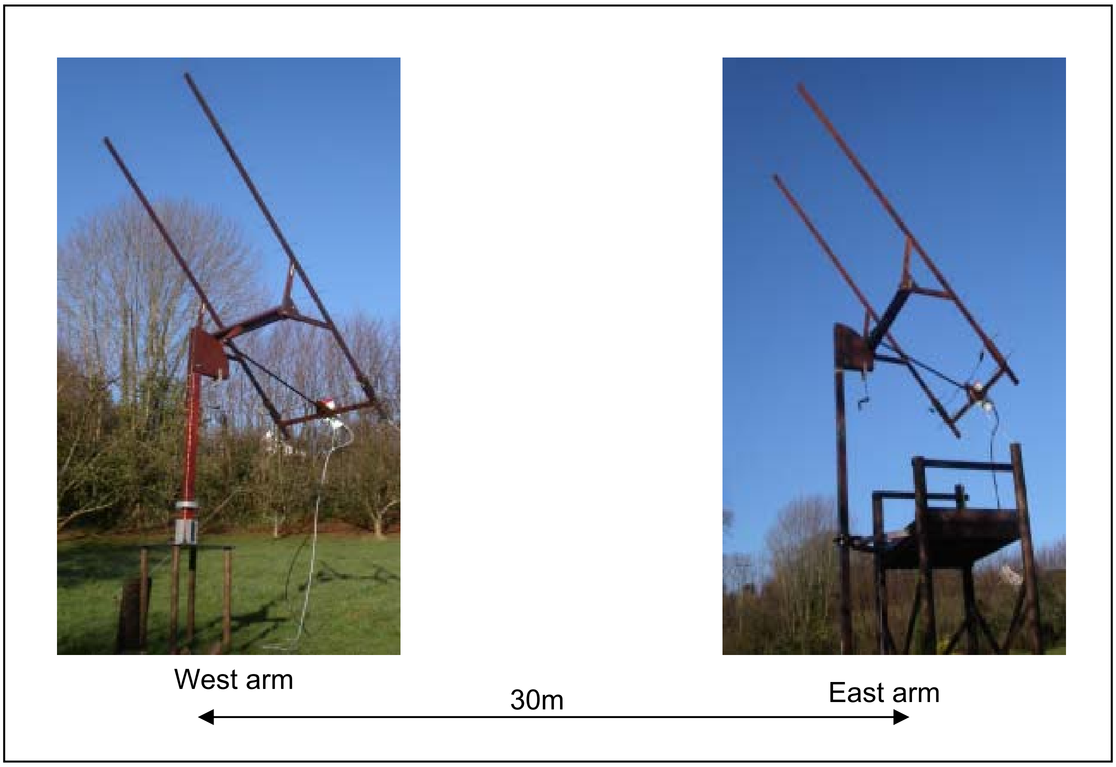

Figure 6 Photographs of 408MHz interferometer antennas

2.3 Antenna elements

Each arm of the interferometer is made from two SARA Quagi antennas stacked 1.2 m apart. The details of construction of a single SARA Quagi can be found at http://www.bambi.net/sara/AntConst.pdf .

Figure 7 A single SARA Quagi

*Society of Amateur Radio Astronomers

This excellent, easy to build antenna is constructed from good quality wood and brass brazing rods for the elements. The calculated performance of the design is shown in Figure 8.

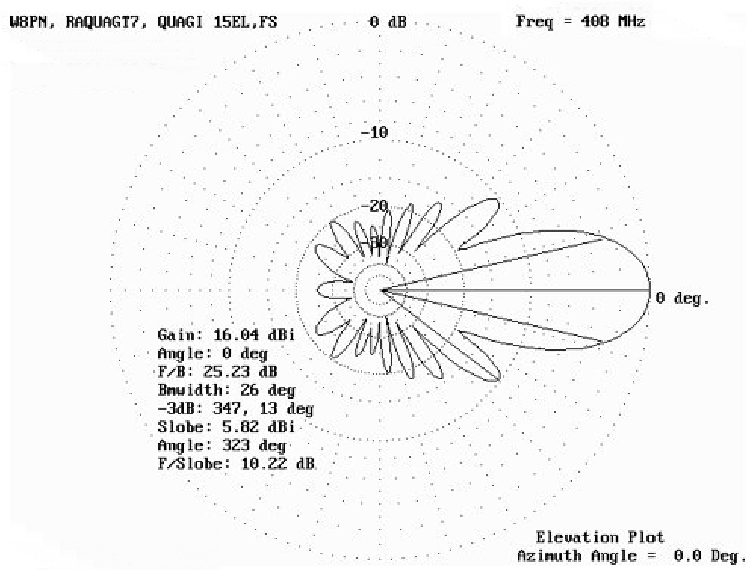

An **amimuth** pattern plot of the 408 Mhz design.

Figure 8 Calculated Antenna Polar Diagram

Considerable work was involved in determining the optimum distance to stack two of these antennas in order to obtain a single beam with a narrower width than each element on its own. This narrowing of the beam helps in confining the spread of the interferometer fringes (as shown in Figure 5) to help reduce the generation of multiple fringe patterns from more than one source that may be in the wide beam of a single antenna arm.

Experiments were carried out using an 'antenna range' in a large flat field with a small 408MHz signal source in the far field some 50m from the antenna being tested as shown in Figure 9.

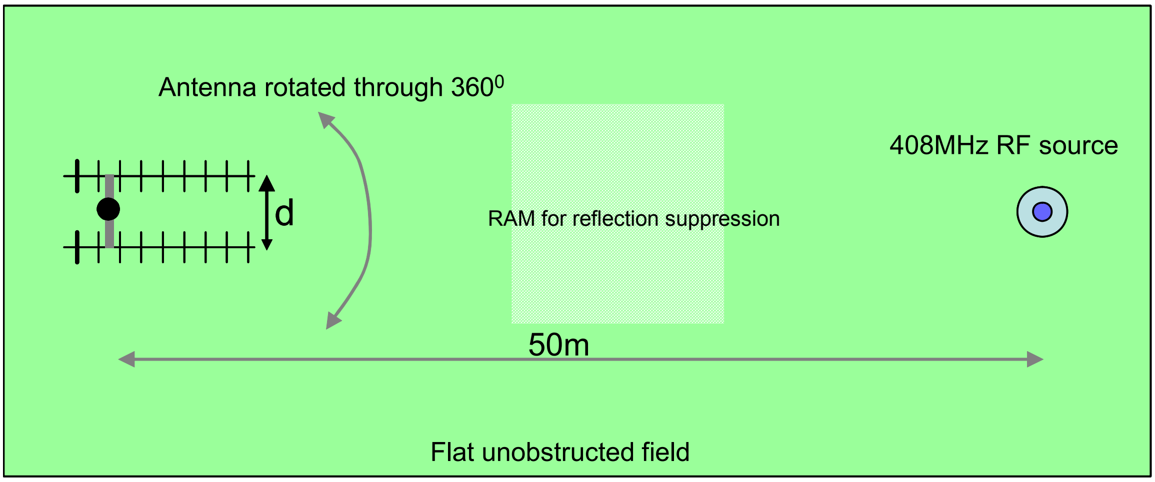

Figure 9 Polar diagram measurements on an antenna range

Polar responses were measured as function of antenna element separation **d** over the range 0.5m to 2m with the best results being at 1.2 separation. Figure 10 shows the measured response of the two stacked Quagis indicating a clean main beam with the first sidelobes > 14dB down.

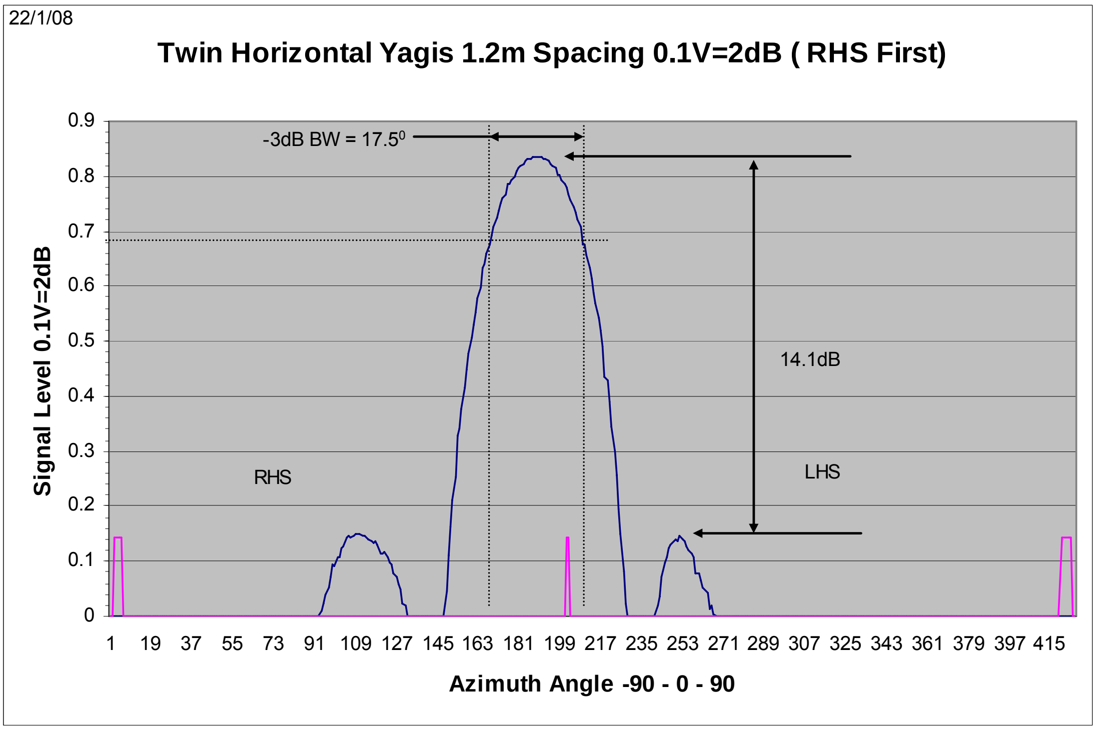

Figure 10 Measured response of stacked Quagis with 1.2m separation

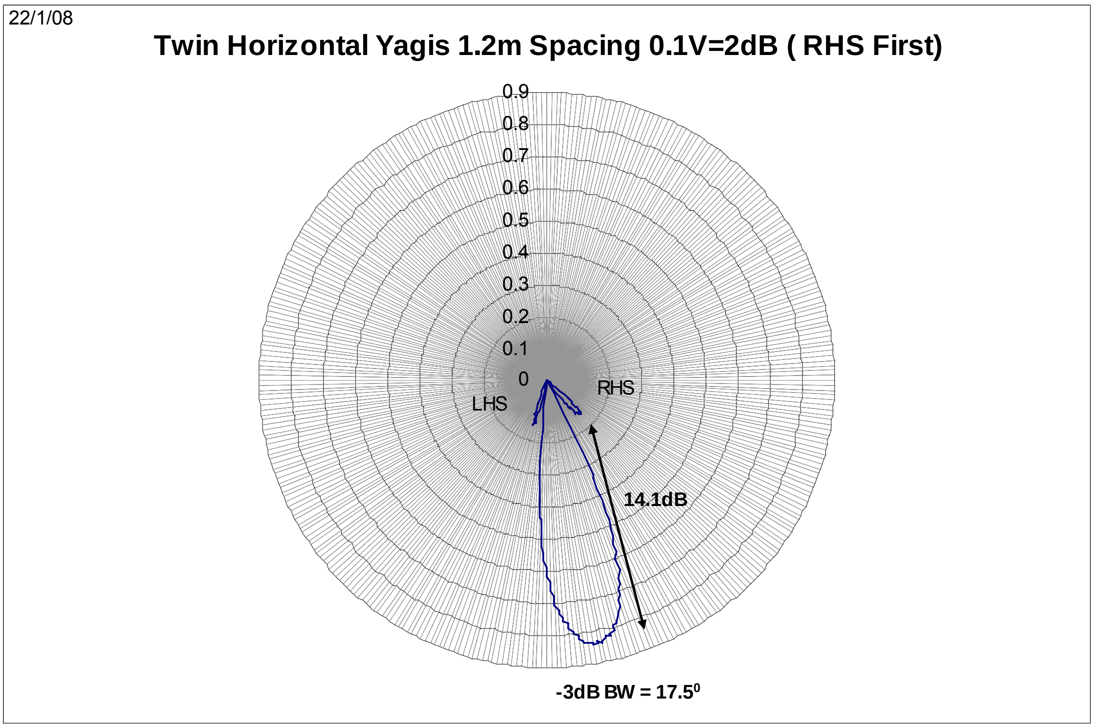

Figure 11 Polar diagram of stacked Quagis with 1.2m separation

The data in Figure 10 can be converted to a polar plot as shown in Figure 11. To obtain these results the antenna being measured is mounted on an antenna rotator and stand a couple of wavelengths above the ground in a similar manner to that shown in Figure 12.

Figure 12 Antenna on a rotating stand being measured

2.4 Receiving system

It is not the intention here to give a full account of the receiving system as it would make this report overlong. The most important component is the temperature controlled Low Noise Amplifier (LNA) mounted on each antenna arm of the interferometer. Its construction is shown in Figure 13.

The unit is enclosed in a weatherproof, thermally-insulated plastic tube that is located between the Quagi antennas on the joining arm support as shown in Figure 14.

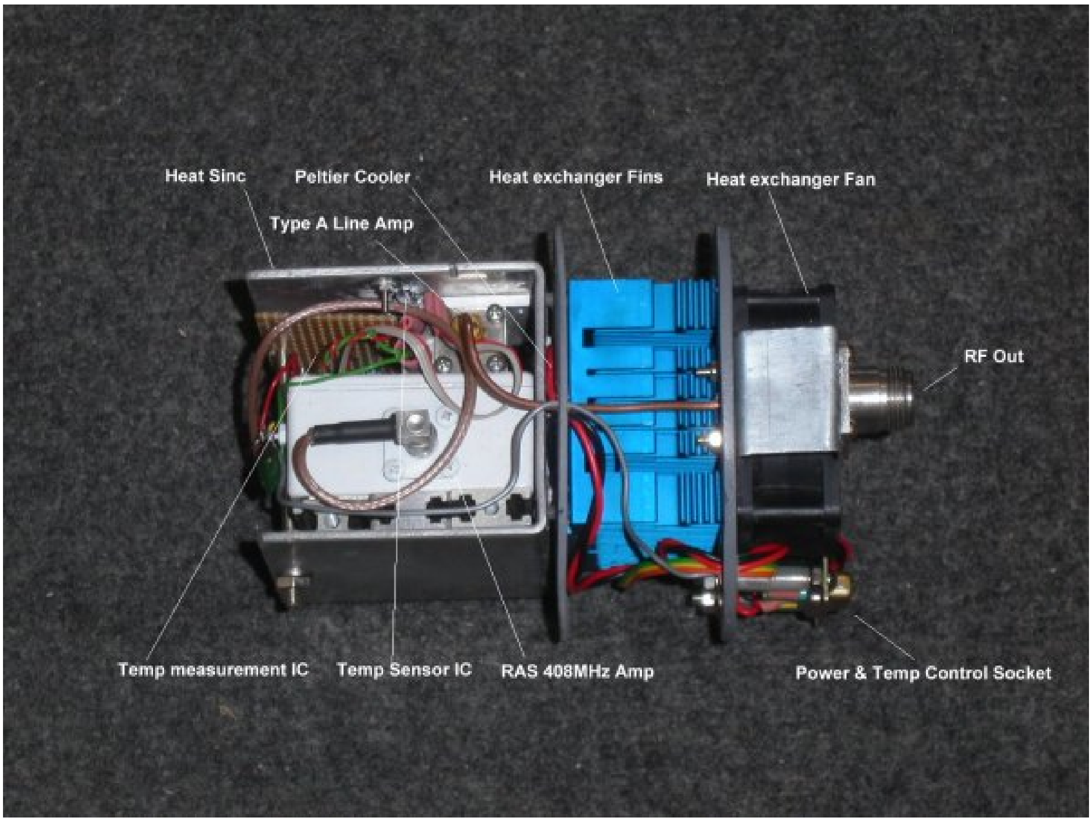

Figure 13 Temperature controlled Head Amplifiers

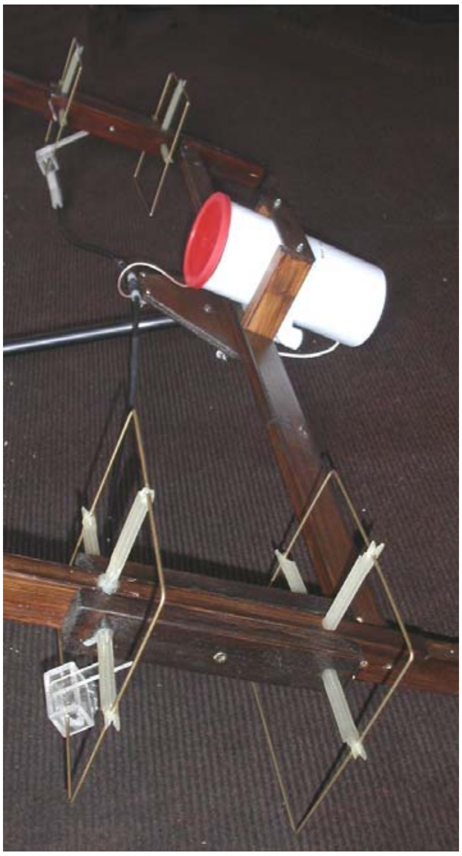

Figure 14 (to the left) shows the head amplifier mounted between the Quagis and connected to the active elements by a cable based combiner using lengths of 50Ω and 75Ω coaxial cable.

The head amplifier contains a RAS 408MHz LNA [8] and an 18dB gain MMIC line driver giving a total stabilised gain of 44dB.with a noise figure of 0.35dB. See Figure 15.

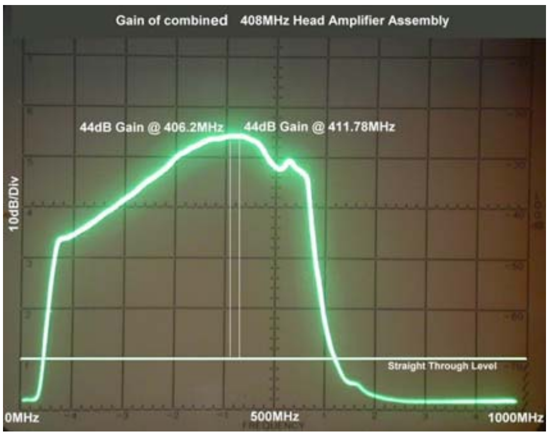

Figure 15 Gain of Head Amplifier Unit

3 Observation of Virgo A

3.1 Virgo A location and beam pointing

When attempting to detect a weak source such as Virgo A, it is vital to have some aid to pointing the antenna beam in the correct direction. The Radio Eyes software [9] is invaluable. A screen shot showing the location of Virgo A and the size of the interferometer main beam is given in Figure 16.

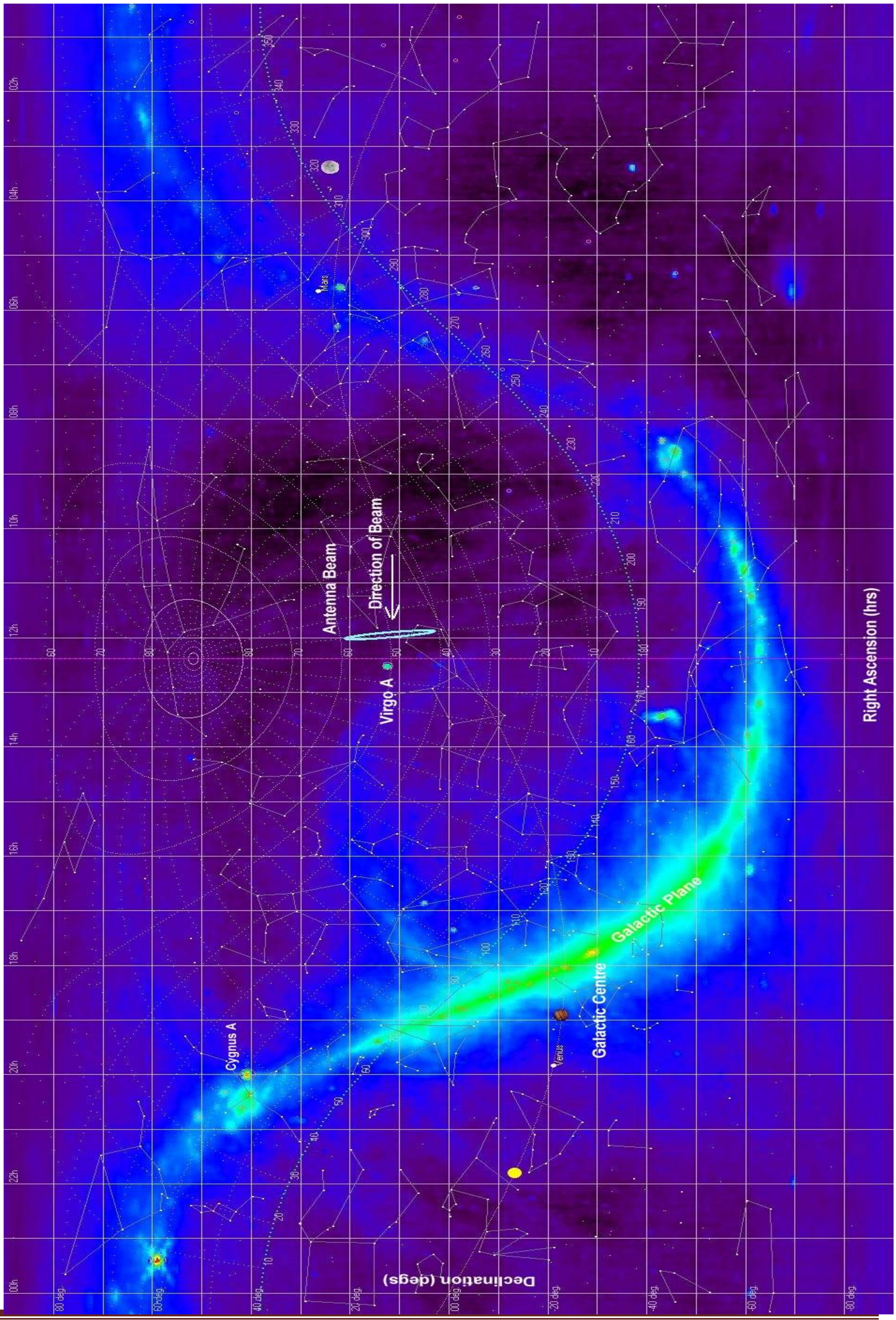

Figure 16 Radio Eyes map of sky @ 408MHz

From Figure 16 it can be seen that it is fortunate that the Virgo A radio source lies well out of the galactic plane - toward the north galactic pole - as this enables it to be detected without clutter from the widely dispersed Galactic noise.

The relevant detail around Virgo A from Figure 16 is presented in Figure 17. Here we see the central interferometer beam positioned to cross Virgo A in about 1 hour's time as the Earth rotation sweeps the beam from right to left in this diagram. The east and west interferometer antennas are elevated at 50^0 and pointing due south for the transit.

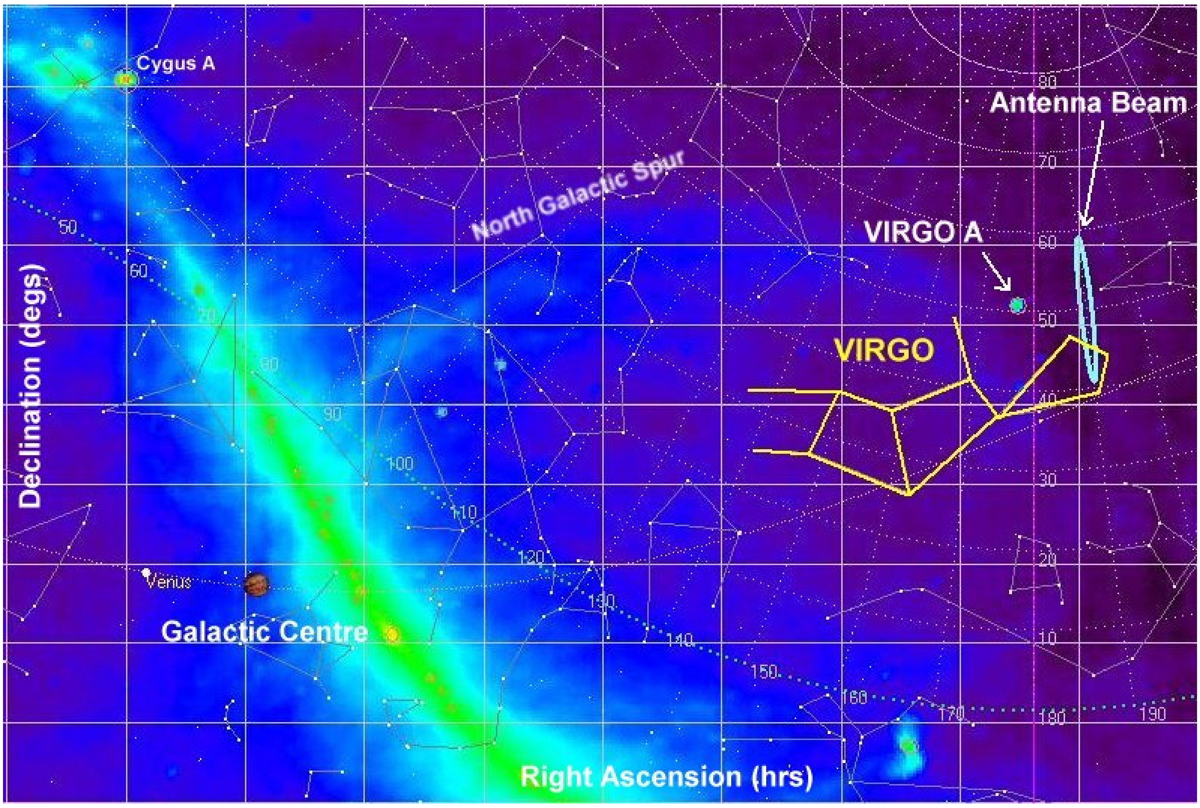

Figure 17 Detail of transit measurement of Virgo A

Of course, the situation is more complex than shown above because the interferometer beam pattern has subsidiary beams on either side of the main central beam as depicted in Figure 5 in section 2.2. The gain of the central beam is a maximum, with those to either side decreasing in gain at increasing angular separation. This leads to a gently increasing pattern of peaks until the maximum is reached - followed then by a gentle decrease until the signal is no longer detectable.

This can be visualized as shown in Figure 18 and demonstrates how the 'beams' produce the received signal strength variation called the 'fringe pattern'.

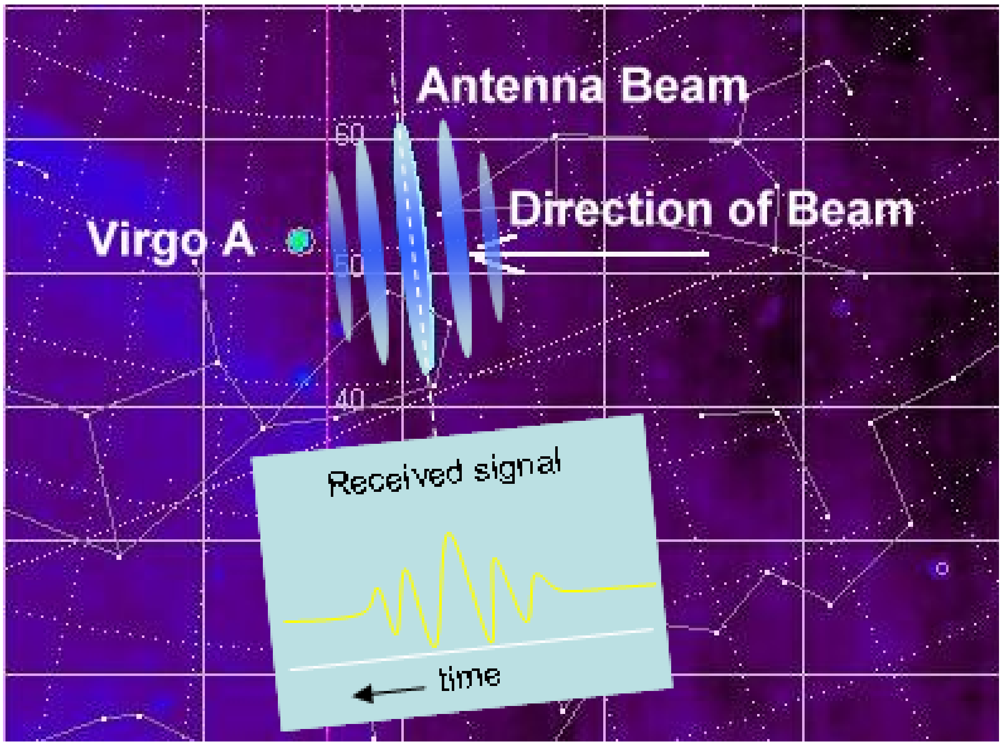

Figure 18 Beams move through the source generating 'fringe pattern'

The angle separating the beams in this interferometer is 1.4^0, which means that as the earth rotates at 15^0 / hour the source passes through one of the interferometer beams in approximately 1.4 x 60/ 15 = 5.6 minutes. Thus the time between peaks in the received signal pattern is 5.6 minutes as shown in Figure 19. This is known as the fringe frequency.

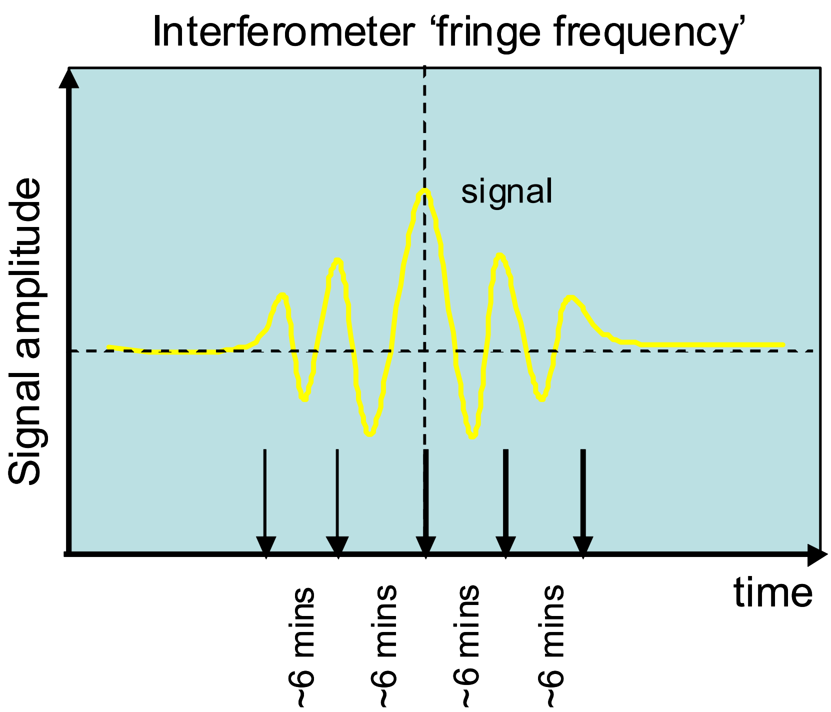

Figure 19 Plot of time between received signal maxima

3.2 Interferometer resolution and object size

The description given above of the operation of a radio interferometer applies if the angular dimension of the source object is smaller than the angular resolution of the interferometer. In this case clear signal fringes are formed as the 'point source' object moves through the beams. Traditionally interferometers have been used to measure the angular dimensions of small sources by increasing the length of the baseline until recognisable fringe patterns disappear. At this point the interferometer can be said to have resolved the source. In professional measurements resolutions of minutes or seconds of arc have been achieved.

When an interferometer is pointed toward an extended radio source (where its angular dimensions are greater than the interferometer resolution) no fringes will be observed and the receiver will revert to a 'total power' measurement. This occurs because there are signals from different parts of the source P1,2,3 to Pn being received by multiple antenna beams at any one time which 'smoothes out' the fringe pattern. See Figure 20.

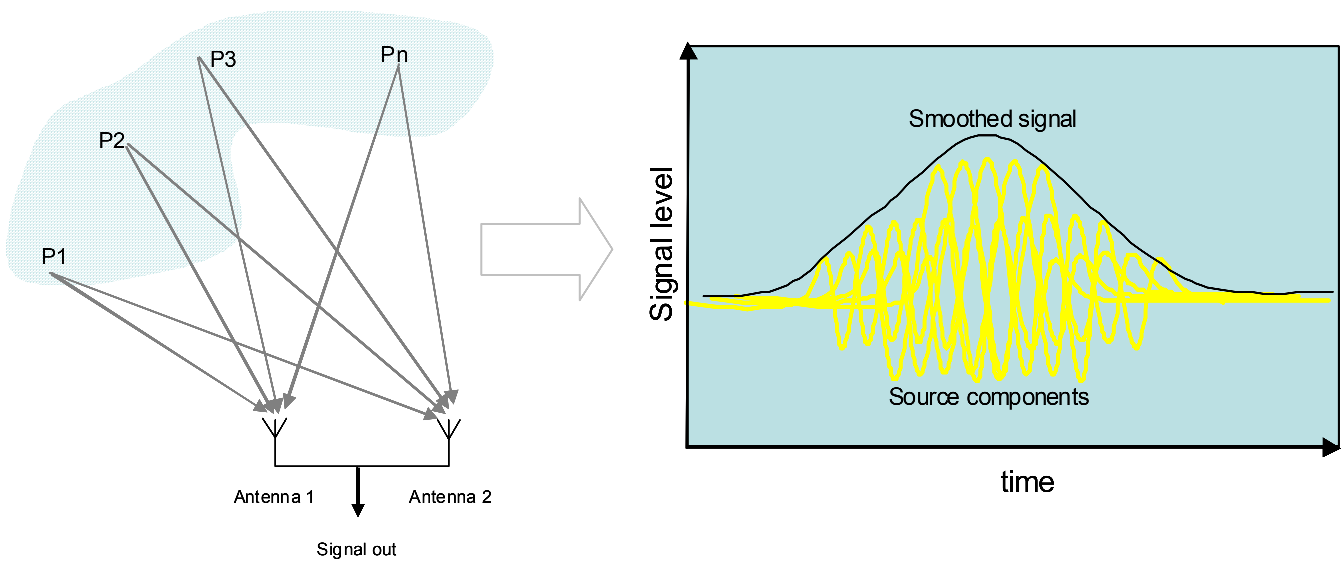

Figure 20 Distributed source results in smoothed out fringes

The contribution from regions P1 to Pn of the extended source all produce fringes which overlap each other, 'filling in' the pattern and resulting in a smoothed signal with time as the large source moves through the sky.

An example of this will be seen in the results section of this article (Figure 21) where the signal from the extended emission from the Milky Way is recorded as a smoothly varying signal and that from the 'point source' of Virgo A shows small but characteristic fringes.

3.3 Results

Measurements were made with the 30m baseline interferometer at 406.5MHz* during nighttimes in February 2008. The winter months are good for measurements because the temperature is usually low and relatively stable overnight. This makes the operation of the temperature control of the LNAs in the head amplifiers easier to achieve. The selected source Virgo A is also visible and at a reasonable high elevation of 50^0 which avoids thermal radio noise from the ground entering the antenna beam.

The result of a measurement made on 13/2/08 is shown in Figure 21.

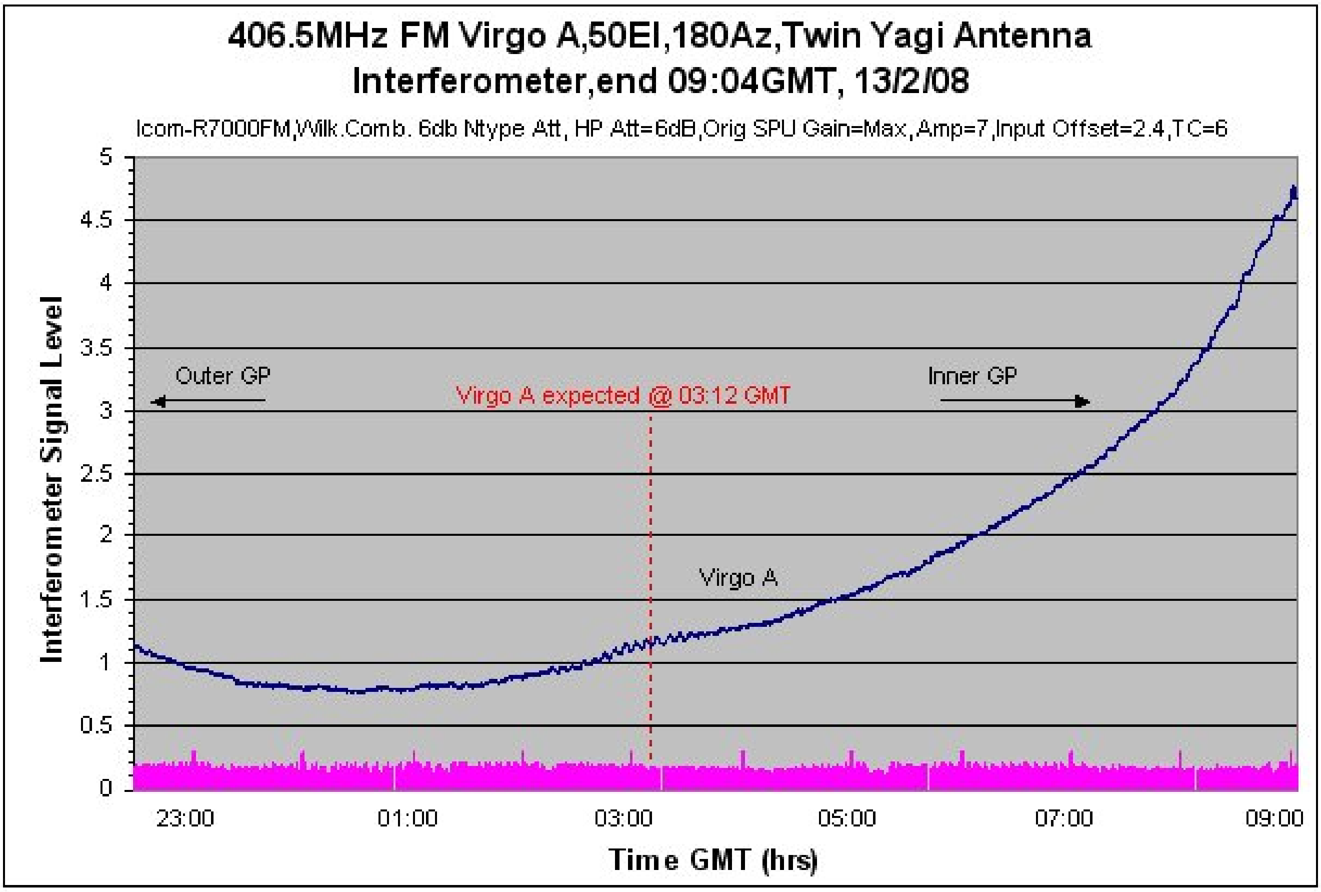

Figure 21 Signal record from 30m baseline interferometer at 406.5MHz

The main feature of this record is the high intensity slowly varying signal (blue trace) over the period of the measurement from ~ 23:00 to ~09:00hrs. This is due to the distributed emissions within the Milky Way and shows a dip as the antenna beam moves away from the outer edge of the galactic plane toward the North Galactic Pole and then back in toward the inner region of the galactic plane. This movement of the beam, out of and into the Galactic plane can be seen in Figure 16.

*This frequency was chosen to be within the bandwidth of the antenna / receiver but free of interference.

At approximately 03:12hrs when Virgo A is expected to pass through the interferometer beam we can see the tell-tale fringe pattern indicating the presence of a small diameter source. The transit time of Virgo A is predicted by the Radio Eyes software and the actual transit is in close agreement.

It is obvious that the signal from Virgo A is much smaller than that from the Milky Way and confirms that it is a challenging object for the amateur radio astronomer to detect. With such a small signal the receiver system noise level and the gain stability of the equipment is of key importance to being able to 'see' this source.

With sufficient long term stability it is possible to process and combine records obtained on different days to improve the signal to noise ratio and bring out the fringe pattern features. This has been done to produce the record shown in Figure 22 clearly indicating the detection of Virgo A.

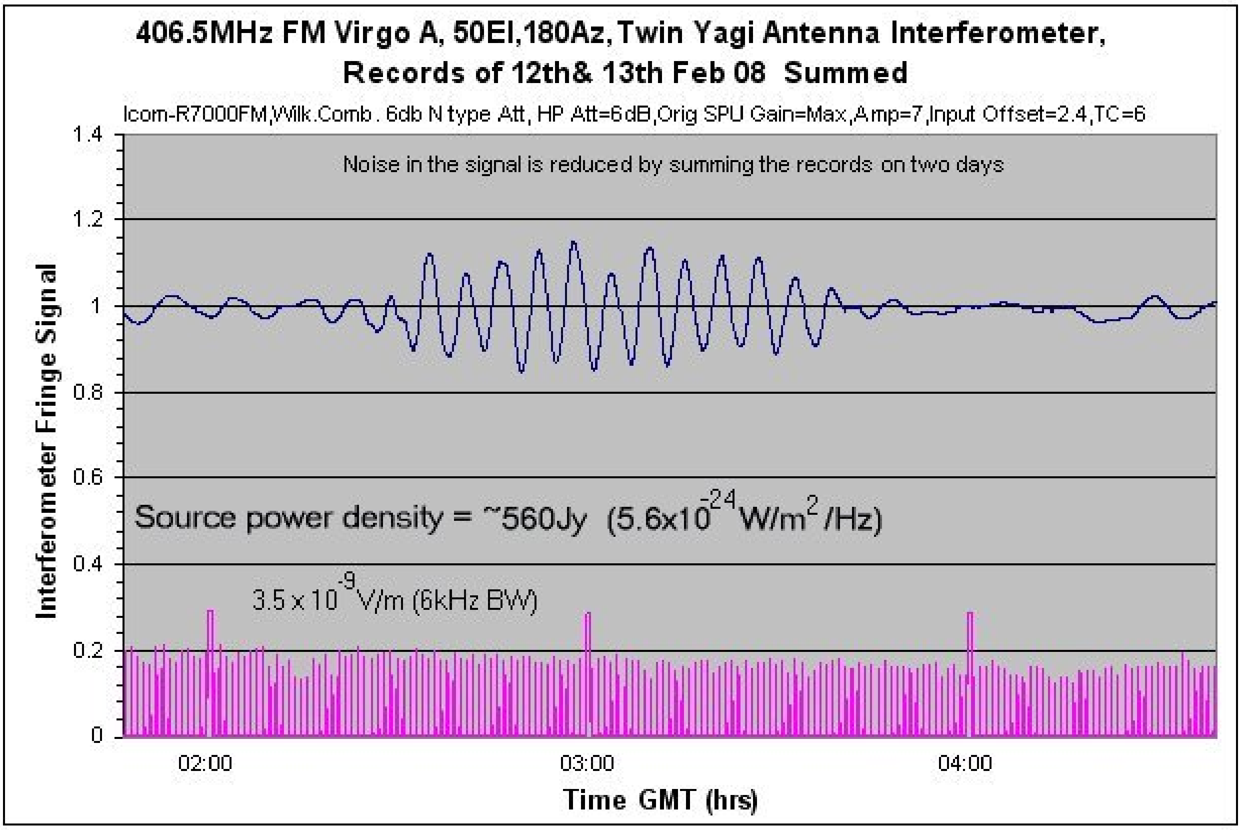

Figure 22 Processed interferometer record of Virgo A detection

The signal shown in Figure 21 is processed using EXCEL spreadsheet calculations to remove the Galactic background component to leave the Virgo A fringe pattern. Two such data sets are then combined to yield the result in Figure 22 which represents the final output of the measurement process. It is interesting to note that the field strength at the antenna is only a few thousands of a millionth of a Volt / metre.

4 Conclusions

It is possible for an amateur radio astronomer to detect this extragalactic object, although it represents a real challenge to achieve the required sensitivity and stability of the measurement equipment.

Interferometry is probably the best technique for the amateur to use as the antennas can be manufactured and mounted on a long baseline for a reasonable budget. The cost of a large dish to obtain equivalent sensitivity is probably beyond the scope of many amateurs.

Using an interferometer also has the benefit of differentiating 'point sources' lying outside our galaxy from the more intense widely dispersed radio noise from the Milky Way.

5 References

1. David Malin of the Anglo-Australian Observatory
2. seds.org/messier/m/m087.html
3. Macchetto, F.; Marconi, A.; Axon, D. J.; Capetti, A.; Sparks, W.; Crane, P. (November 1997). "The Supermassive Black Hole of M87 and the Kinematics of Its Associated Gaseous Disk". *Astrophysical Journal* **489** (2): 579. arXiv:astro-ph/9706252. Bibcode 1997ApJ...489..579M. doi:10.1086/304823.
4. Di Matteo, Tiziana; Allen, Steven W.; Fabian, Andrew C.; Wilson, Andrew S.; Young, Andrew J. (January 2003). "Accretion onto the Supermassive Black Hole in M87". *The Astrophysical Journal* **582** (1): 133–140. arXiv:astro-ph/0202238. Bibcode 2003ApJ...582..133D. doi:10.1086/344504.
5. J S Hey The Radio Universe Pergamon Press pp 50 – 62
6. John Fielding Amateur Radio Astronomy RSGB Pub. Pp 153- 163
7. http://www.bambi.net/sara/AntConst.pdf
8. www.**radioastronomysupplies**.com
9. www.**radio**sky.com/**radioeyes**ishere.html

Dr David Morgan

www.dmradas.co.uk